Geophysical Research Letters

RESEARCH LETTER
10.1029/2018GL079615

Key Points:
- We identified 163 SAR arc detachment events in 2006-2016 at subauroral latitudes
- SAR arc detachment can be an important indicator of ring current particle injection
- SAR arc detachments tend to occur at the beginning of a substorm recovery phase

Correspondence to:
K. Shiokawa,
shiokawa@nagoya-u.jp

Citation:
Takagi, Y., Shiokawa, K., Otsuka, Y., Connors, M., & Schofield, I. (2018). Statistical analysis of SAR arc detachment from the main oval based on 11-year, all-sky imaging observation at Athabasca, Canada. *Geophysical Research Letters*, *45*, 11,539–11,546. https://doi.org/10.1029/2018GL079615

Received 13 JUL 2018
Accepted 17 OCT 2018
Accepted article online 22 OCT 2018
Published online 5 NOV 2018

Statistical Analysis of SAR Arc Detachment From the Main Oval Based on 11-Year, All-Sky Imaging Observation at Athabasca, Canada

Yuki Takagi[1], Kazuo Shiokawa[1], Yuichi Otsuka[1], Martin Connors[2], and Ian Schofield[2]

[1] Institute for Space-Earth Environmental Research, Nagoya University, Nagoya, Japan, [2] Athabasca University Observatories, Athabasca University, Athabasca, Alberta, Canada

Abstract We report the first statistical analysis of stable auroral red (SAR) arc detachments from the main auroral oval, using 630-nm all-sky cooled-Charge Coupled Device images obtained at Athabasca (magnetic latitude = 61.7°N), Canada. SAR arc detachments from the main oval can be an important way of monitoring the characteristics of ring current particle injection in the inner magnetosphere. We analyzed all-sky images obtained for 11 years from 2006 to 2016 and found 163 SAR arc detachment events. The SAR arc detachments tend to occur in the premidnight sector, indicating the ring current ion drift to the dusk sector. The SAR arc detachments also tend to occur at the beginning of the substorm recovery phase, suggesting that the SAR arcs detach from the main oval as the main auroral oval returns to higher latitudes. The equatorward velocities of detached SAR arcs are from −100 m/s (poleward) to +200 m/s (equatorward), corresponding to magnetospheric electric fields from −1 to +2 mV/m.

Plain Language Summary Stable auroral red (SAR) arcs are the optical emissions caused by low-energy electron precipitation into the ionosphere from the inner magnetosphere close to the earth. In this paper, we report the first statistical analysis of SAR arc detachments from the main auroral oval, using all-sky cooled-Charge Coupled Device images measured at a wavelength of 630.0 nm obtained at Athabasca, Canada, which is located at latitudes just lower than the auroral zone latitudes. SAR arc detachments from the main oval can be an important way of monitoring the characteristics of high-energy particle injection in the inner magnetosphere. We analyzed 11-year all-sky images from 2006 to 2016 and found 163 SAR arc detachment events. The SAR arc detachments tend to occur premidnight, indicating the high-energy ion drift to the dusk sector. We also found that the SAR arc detachments tend to occur at the beginning of the substorm recovery phase. This likely indicates that the SAR arcs detach from the high-latitude aurora as the main aurora returns to higher latitudes at the beginning of the recovery phase. The equatorward velocities of detached SAR arcs are also estimated from the analysis.

1. Introduction

A stable auroral red (SAR) arc is an optical phenomenon caused by low-energy electron precipitation from the magnetosphere at subauroral latitudes (e.g., Cole, 1965; Kozyra et al., 1987; Mendillo et al., 2016; Rees & Roble, 1975). It occurs when the plasmasphere expands outward during the recovery phase of a magnetic storm. High-energy plasma in the ring current heats the low-energy plasma in the plasmasphere through Coulomb collisions and wave-particle interactions. The heated electrons in the plasmaphere fall into the ionosphere at subauroral latitudes along magnetic field lines. This heats electrons in the *F* layer at altitudes of ~400 km, exciting the O (^{1}D) state to generate red emission at a wavelength of 630.0 nm.

It has been shown that SAR arcs occur during the recovery phase of geomagnetic storms (e.g., Kozyra et al., 1987; Mendillo et al., 2016; Rees & Roble, 1975). Shiokawa et al. (2013) reported red aurora that seemed to be SAR arc at low latitudes in Japan when the ring current developed at the beginning of a magnetic storm. Baumgardner et al. (2007) reported a rare SAR arc with a very bright intensity reaching 13,000 Rayleigh. Mendillo et al. (2016) reported SAR arcs observed for more than 24 hr at widely separated stations. Mendillo et al. (2016) classified SAR arcs into five categories according to their forms and discussed possible mechanisms. These SAR arcs occur during geomagnetic storms and also can be related to storm time substorms.

Recently, Shiokawa et al. (2009) reported a SAR arc detachment from the main oval during nonstorm time substorms. The SAR arc detachment from the main auroral oval may relate to the characteristics of ring current particle injection in the inner magnetosphere and could be an important tool to monitor the state of high-energy plasma in the inner magnetosphere. However, a statistical analysis of such SAR arc detachment has not yet been done. In this study, we analyzed SAR arc detachment from the main oval based on 11 years of auroral observation from 1 January 2006 to 31 December 2016 at Athabasca, Canada. We performed a statistical analysis of the SAR arc detachment with reference to their magnetic local time (MLT) distribution, yearly variation, and equatorward velocities and in relation to the AU/AL/SYM-H indices.

2. Observation

In this study, we used auroral images obtained by the all-sky camera no. 7, which was installed on 3 September 2005 in Athabasca (54.7°N, 118.3°W, magnetic latitude: 61.1°N, $L = 4.3$), Canada, as part of the Optical Mesosphere Thermosphere Imagers (Shiokawa et al., 1999, 2000). Since the station is close to the auroral oval at subauroral latitudes, we can observe SAR arc detachment during nonstorm time substorms. Although we use a cooled-Charge Coupled Device camera with 512×512 pixels, the obtained images had a resolution of 256×256 pixels after 2×2 binning to increase the sensitivity of the camera. This camera had six band-pass filters that allowed measurement of airglow/auroral emissions at specific wavelengths (OI [557.7 nm], OI [630.0 nm], Hβ [486.1 nm], Na [589.3 nm], OH bands [20–910 nm], OI [844.6 nm], and background [572.5 nm]). In this study, the band-pass filter at 630.0 nm was used to image the SAR arcs, which are caused by the emission of oxygen atoms in the *F* layer. We also examined the images collected through the band-pass filter at 557.7 nm to see the emission caused by higher-energy particle precipitation. These images are obtained with a time resolution of 2 min. The all-sky images contain background continuum emission throughout the transmission width of the band-pass filter. We removed the background emission using images collected through the band-pass filter at 572.5 nm. Additionally, we projected all-sky images passed through a fish-eye lens on the geographical latitude/longitude coordinates by assuming that the emission altitude was 400 km for 630 nm and 120 km for 557.7 nm. By mapping these images onto geographical coordinates, it was possible to measure north-south cross sections with time (keogram) representing the time change of the auroral emission intensities and their latitudinal motion.

Figure 1 shows examples of SAR arc detachment keograms observed in Athabasca at a longitude of 118°W. Figures 1a–1c show the keograms observed through the 630.0-nm filter, and Figures 1d and 1e show examples of simultaneous observation using the 630.0- and 557.7-nm filters. The vertical axis is shown in geographic latitudes. The geomagnetic latitudes are $\sim +6°$ of geographic latitudes. In Figures 1a–1c, SAR arc detachment from the auroral oval at high latitudes can be observed. The SAR arc seen in Figure 1d was hardly seen in the keogram at 557.7 nm (Figure 1e), indicating a narrow emission bandwidth centered near 630.0 nm. In the sky above Athabasca, this type of SAR arc, which is detached from the main oval, was typically observed. Therefore, in this study we performed statistical analysis on the SAR arc detachment from the main oval.

3. Statistical Analysis

In this study, we used keograms with a color scale of 0–500 R, as shown in Figure 1, and determined the occurrence of SAR arc detachment based on visual inspection under the following criteria: (1) intensification and lower-latitude expansion of high-latitude aurora and subsequent separation of SAR arcs in the 630-nm keogram and (2) the 557.7-nm keogram does not show strong emission at the corresponding arc location, indicating that the 630-nm emission is the dominant emission of the arc. (3) We also checked movies of 630-nm all-sky auroral images to check that the structures picked up from the keograms are east-west elongated arcs detaching from the main oval auroras. Using these criteria, 163 events of SAR arc detachment were found from 1 January 2006 to 31 December 2016. Mendillo et al. (2016) studied 314 SAR arcs obtained from 27 years (12 events per year). Thus, the SAR arc detachment events occur more frequently compared with storm time SAR arcs.

Three parameters were extracted from these 163 events: start time, end time, and the lowest latitude. The start time was defined as the time when the SAR arc started to detach from main oval in the keogram, and the end time was defined as the time when the emission disappeared or was masked by other auroral activities or clouds. The lowest latitude is the minimum latitude that the detached SAR arc reached.

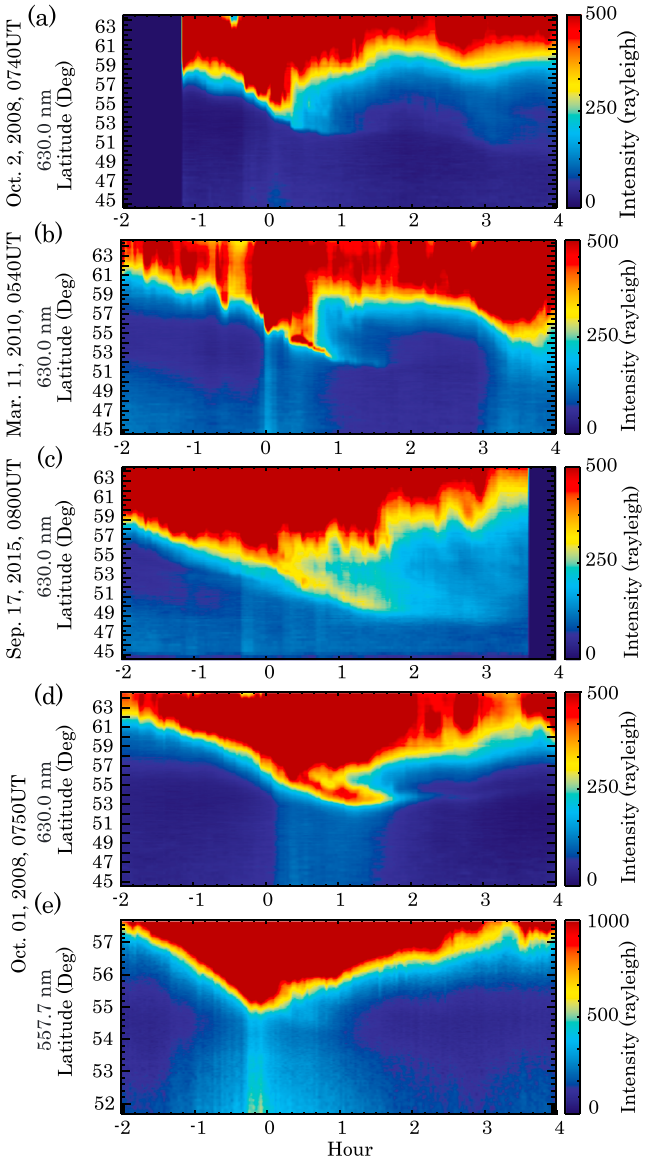

Figure 1. Example keograms showing stable auroral red arc detachment from the main auroral oval at high latitudes. They were measured at 630.0 nm on (a) 2 October 2008, (b) 11 March 2010, (c) 17 September 2015, and (d) 1 October 2008. In (e), a keogram measured at 557.7 nm on 1 October 2008 is shown. The vertical axis is shown in geographic latitudes. The geomagnetic latitudes are ~ +6° of geographic latitudes.

Figure 2a shows the occurrence rate of SAR arc detachment as a function of MLT. The numbers above each time represent the total time (hours) of observation with clear sky at Athabasca. The occurrence rate was calculated by dividing the number of SAR arc detachment by these total observation time. In other words, we counted the hourly bin with SAR arc detachment and divided it by the total observation hours to define the occurrence rate. The occurrence rate is highest at 20–22 MLT, before midnight. Figure 2b shows the yearly variation of the SAR arc occurrence rate, geomagnetic Ap index, and the solar F10.7 flux. The Ap index and the F10.7 flux are 1-year averages. The SAR arc occurrence rate is generally low at the solar minimum and increases toward the solar maximum, though there are 2 years with low occurrence rates at the solar maximum. Thus, the occurrence rate correlates better with the Ap index. Figure 2c shows the distribution of the SAR arc duration. The horizontal axis shows the duration, and the vertical axis shows the number of events, indicating that the typical duration for a detached SAR arc is 1–2 hr. However, it should be noted that this duration is determined by the measured end time, which can be triggered prematurely by the termination of

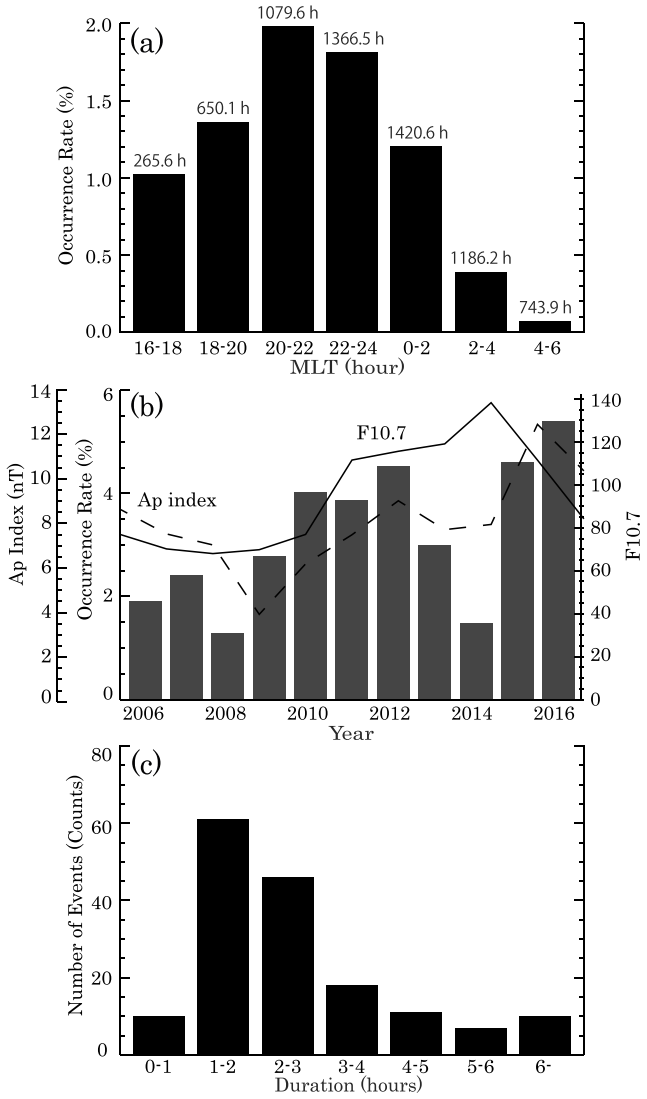

Figure 2. The occurrence rate variation of detached SAR arcs against (a) MLT and (b) year with Ap index and the solar 10.7 flux. (c) The distribution of the duration time of a detached SAR arc. MLT = magnetic local time; SAR = stable auroral red.

camera operation due to Sun/Moon rise or masking of the signal by clouds or other auroral activity. Therefore, the actual duration of a detached SAR arc could be longer than that shown in Figure 2c.

Figure 3 shows the results of superposed epoch analysis of (a) AU and AL indices and (b) the SYM-H index from 2 hr before to 4 hr after the SAR arc detachment. These parameters are provided by the World Data Center for Geomagnetism, Kyoto University, Japan, through the OMNI database. The average values defined every 1 min are indicated by the solid lines, and the standard deviations for every 30 min are indicated by the error bars. The AL index begins to decrease at ~1 hr before the time of SAR arc detachment, with its minimum value occurring around the detachment time. This suggests that the SAR arc detachment occurs when the substorm recovery phase starts. On the other hand no clear change in the SYM-H index is observed before or after the SAR arc detachment. The average value of the SYM-H index remains near −20 nT, indicating that the SAR arc detachment is likely to occur during geomagnetically disturbed periods.

The detached SAR arcs tend to move to low latitudes. Since the position of a SAR arc is an ionospheric mapping of the position of energetic ions in the magnetosphere, there is a possibility that the equatorward velocity of the detached SAR arcs indicates the inward velocity of high-energy ions in the magnetosphere. The equatorward velocity of a SAR arc was estimated from the change in the latitude of the SAR arc peak intensity at

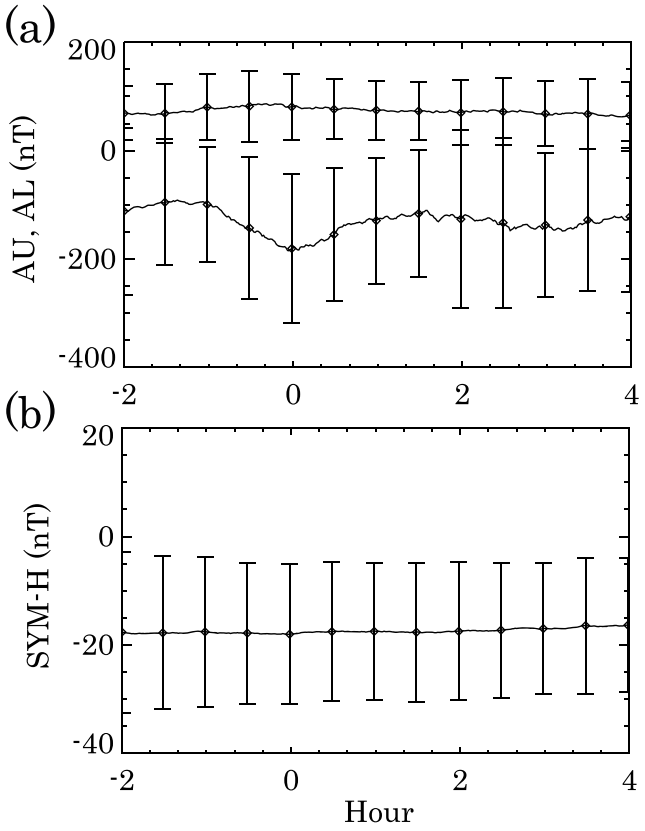

Figure 3. The superposed epoch analysis of stable auroral red arc detachment for (a) AU, AL indices and (b) SYM-H index. The zero time is at the point of stable auroral red arc detachment.

0.5 and 1 hr after the SAR arc detachment time. We analyzed 76 cases of detached SAR arcs from among the total of 163 cases by excluding events with duration less than 1 hr. Figure 4a shows the relationship between the estimated equatorward velocity and MLT. The velocity is distributed between −0.1 km/s (poleward) and +0.2 km/s (equatorward). The equatorward velocities of SAR arcs tend to be higher in the dusk and dawn local times compared with those around midnight. From Figure 4b, no significant relationship was seen between the velocity and the geomagnetic activity, as represented by the SYM-H index (correlation coefficient: −0.17). The estimated equatorward velocities in the ionosphere were then projected to the inward velocity in the magnetosphere using the Tsyganenko-06 model (Tsyganenko, 2006), and the magnetospheric westward electric field was estimated by assuming that the equatorward motion of the SAR arc is caused by the inward E × B drift in the magnetosphere. The estimated westward electric fields in the magnetosphere are ∼0–2 mV/m, as shown in Figure 4c. The electric field becomes stronger in the dusk and dawn local times, similar to that of SAR arc velocity in the ionosphere.

4. Discussion

In Figure 2a, it was shown that the occurrence rate of SAR arc detachment was highest in 20–22 MLT. This could be due to the duskward drift of the ring current ions, which are the energy source of a SAR arc. This premidnight to dusk preference of SAR arc detachment is similar to that of Subauroral Polarization Stream and Subauroral Ion Drift, which are also occurring at subauroral latitudes during substorms and storms. Spatial and temporal association between SAR arcs and Subauroral Ion Drift have been shown by for example, Foster et al. (1994) and Mishin et al. (2004). Correspondence of SAR arc detachment with these subauroral ion-flow structures will be an interesting issue for future study.

In Figure 2b, it can be seen that the occurrence rate of SAR arc detachment was low in the solar maximum and minimum and high during the period of increase or decrease of solar activity. The occurrence rate also correlated well with geomagnetic activities represented by the Ap index. Alexeyev et al. (2009) showed that the occurrence rate of SAR arcs in the solar cycle 23 has a maximum in the declining phase of solar activity

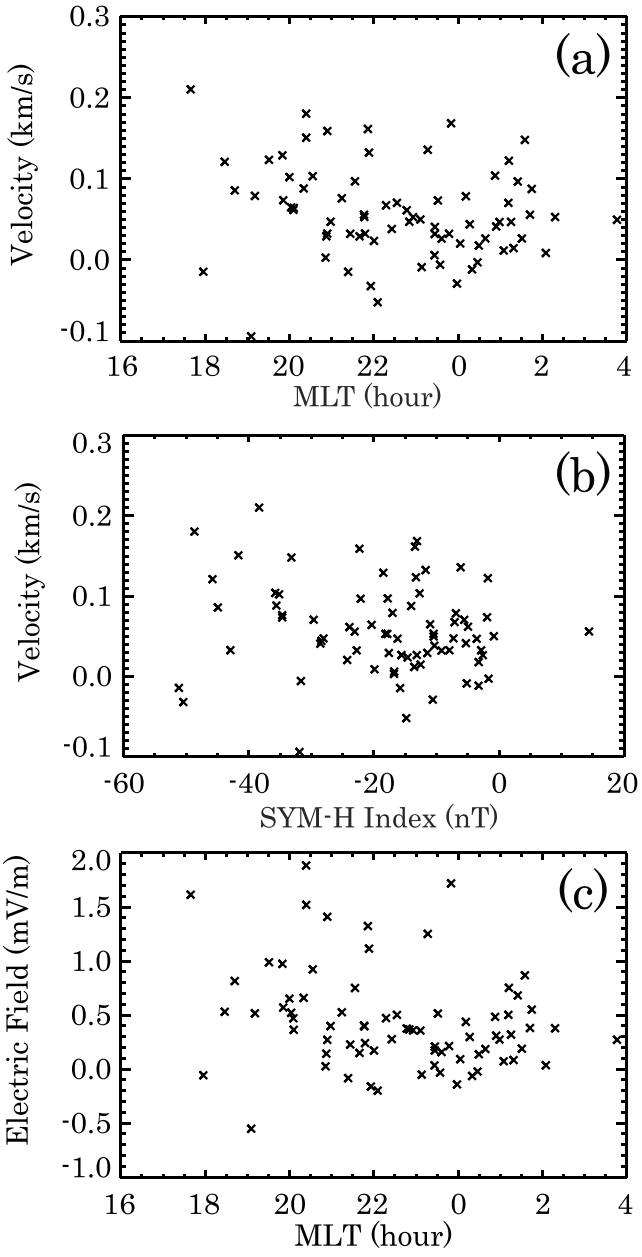

Figure 4. The relationship between (a) the estimated equatorward velocity of detached stable auroral red arcs and magnetic local time (MLT), (b) the estimated equatorward velocity and the geomagnetic activity represented by the SYM-H index, and (c) the projected westward electric field in the magnetosphere against MLT.

and has a good correlation with the Ap index, similar to the present result. Figure 3a shows that SAR arc detachment is likely to occur at the beginning of a substorm recovery phase. It is conceivable that the injection of ring current ions begins at the substorm expansion phase, and the SAR arc detachment from the main oval starts as the main auroral oval returns to high latitudes at the start of the recovery phase.

Detached SAR arcs tend to move equatorward. This equatorward velocity and the associated eastward electric field in the magnetosphere tend to be higher in the dusk and dawn local times. The MLT of SAR arc detachment can be determined by the duskward drift of ring current ions due to the gradient of B and curvature drift. These two drift velocities are proportional to the energy of the ions. When SAR arc detachment appears in the dusk sector, it is expected that the magnetosphere electric field is strong and that ring current ions are accelerated to a higher energy, moving to the dusk side. In that case, the SAR arc velocities toward the equator might be faster because of the stronger magnetospheric electric field. Since SAR arcs are caused by the interaction

between high-energy ions in the ring current and the low-energy electrons in the plasmasphere, it is expected that the electron distribution in the plasmasphere also contributes to the appearance of a SAR arc. However, the equatorward velocity of a SAR arc detachment is considered to be determined by the magnetospheric electric field and not by the electron distribution in the plasmasphere.

In this paper we called the arcs detached from the main oval and characterized by dominant 630-nm emission as the SAR arc detachment. The detachment of these 630-nm dominant arcs seems to be a common phenomenon at the beginning of the substorm recovery phase at subauroral latitudes, as shown in this paper. We should note that for some cases, weak 557.7-nm emission is also accompanied by the observed arc. Thus, our detachment SAR arc may not be pure 630-nm emission. Several previous papers also reported weak 557.7-nm emission during storm time SAR arcs (e.g., Mendillo et al., 2016; Shaeffer & Jacka, 1971).

As shown in Figure 3b, the average SYM-H is about −20 nT, indicating that they are not during geomagnetic storms. The mechanism that causes storm time SAR arcs, that is, spatial overlap of high-energy ring current ions and plasmaspheric low-energy electrons (e.g., Rees & Roble, 1975) may also occur during nonstorm time substorms. Further investigation of magnetospheric satellite data during the SAR arc detachment would be essentially important to understand the mechanism to cause the observed SAR arc detachment.

5. Conclusion

In this study, we performed a statistical analysis of SAR arc detachment from the main oval based on 11 years of all-sky camera observations obtained at subauroral latitudes (Athabasca, $L = 4.3$) from 2006 to 2016. SAR arc detachment from the main auroral oval indicates the situation of ring current particle injection in the inner magnetosphere and can be an important tool for monitoring the state of high-energy plasma in the inner magnetosphere. The following results were obtained from our analysis.

- The yearly variation of SAR arc detachment has a better correlation with the geomagnetic Ap index than the solar F10.7 index.
- The SAR arc detachment tends to occur at premidnight local times, indicating ring current ion drift to the dusk sector.
- The SAR arc detachment tends to occur at the beginning of a substorm recovery phase. This probably indicates that the SAR arcs detach from the main oval as the main auroral oval returns to higher latitudes at the beginning of the recovery phase.
- The equatorward velocities of detached SAR arcs range from −0.1 km/s (poleward) to +0.2 km/s (equatorward), corresponding to the magnetospheric electric field of ∼0–2 mV/m. The equatorward velocities of SAR arcs are higher in the dusk and dawn local times compared with those around midnight. We reason that when the magnetosphere electric field is stronger, the ring current ions are accelerated to higher energies and drift more to the dusk side.

Acknowledgments
We thank Y. Katoh, H. Hamaguchi, Y. Yamamoto, and T. Adachi of ISEE, Nagoya University and Kyle Reiter of Athabasca University for their continuous support of the observation at Athabasca. The optical data obtained at Athabasca are available through ISEE. Quick-look plots of the optical data are available at http://stdb2.isee.nagoya-u.ac.jp/omti/. The construction and operation of the Athabasca University Geospace Observatory (AUGSO) were funded by the Canada Foundation for Innovation. The OMNI data were obtained from the GSFC/SPDF OMNIWeb interface at http://omniweb.gsfc.nasa.gov. The SYM-H, Ap, AU, and AL indices were provided by WDC-C2 for Geomagnetism at Kyoto University. F10.7 was provided by the Natural Resources Canada. This work was supported by grants-in-aid for Scientific Research (15H05815 and 16H06286) provided by the Japan Society for the Promotion of Science.

References

Alexeyev, V., Ievenko, I., & Parnikov, S. (2009). Occurrence rate of SAR arcs during the 23rd solar activity cycle. *Advances in Space Research*, *44*, 524–527. https://doi.org/10.1016/j.asr.2009.04.024

Baumgardner, J, Wroten, J., Semeter, J., Kozyra, J., Buonsanto, M., Erickson, P., & Mendillo, M. (2007). A very bright SAR arc: Implications for extreme magnetosphere-ionosphere coupling. *Annales Geophysicae*, *25*, 2593–2608.

Cole, K. D (1965). Stable auroral red arcs, sinks for energy of main phase. *Journal of Geophysical Research*, *70*, 1689–1706.

Foster, J. C., Buonsanto, M. J., Mendillo, M., Nottingham, D., Rich, F. J., & Denig, W. (1994). Coordinated stable auroral red arc observations: Relationship to plasma convection. *Journal of Geophysical Research*, *99*, 11,429–11,439.

Kozyra, J. U., Shelley, E. G., Comfort, R. H., Brace, L. H., Cravens, T. E., & Nagy, A. F. (1987). The role of ring current O^+ in the formation of stable auroral red arcs. *Journal of Geophysical Research*, *92*, 7487–7502.

Mendillo, M., Baumgardner, J., & Wroten, J. (2016). SAR arcs we have seen: Evidence for variability in stable auroral red arcs. *Journal of Geophysical Research: Space Physics*, *121*, 245–262. https://doi.org/10.1002/2015JA021722

Mishin, E. V., Burke, W. J., & Viggiano, A. A. (2004). Stormtime subauroral density troughs: Ion-molecule kinetics effects. *Journal of Geophysical Research*, *109*, A10301. https://doi.org/10.1029/2004JA010438

Rees, M. H., & Roble, R. G. (1975). Observations and theory of the formation of stable auroral red arcs. *Reviews of Geophysics and Space Physics*, *13*, 201–242.

Shaeffer, R. C., & Jacka, F. (1971). Stable auroral red arcs observed from Adelaide during 1967-69. *Journal of Atmospheric and Terrestrial Physics*, *33*, 237–250.

Shiokawa, K., Hosokawa, K., Sakaguchi, K., Ieda, A., Otsuka, Y., Ogawa, T., & Connors, M. (2009). The optical mesosphere thermosphere imagers (OMTIs) for network measurements of aurora and airglow, future perspectives of space plasma and particle instrumentation and international collaborations. *AIP Conference proceedings*, *1144*, 212–215. https://doi.org/10.1063/1.3169292

Shiokawa, K., Katoh, Y., Satoh, M., Ejiri, M. K., & Ogawa, T. (2000). Integrating sphere calibration of all-sky cameras for nightglow measurements. *Advances in Space Research*, *26*, 1025–1028.

Shiokawa, K., Katoh, Y., Satoh, M., Ejiri, M. K., Ogawa, T., Nakamura, T., et al. (1999). Development of optical mesosphere thermosphere imagers (OMTI). *Earth Planets Space*, *51*, 887–896.

Shiokawa, K., Miyoshi, Y., Brandt, P. C., Evans, D. S., Frey, H. U., Goldstein, J., & Yumoto, K. (2013). Ground and satellite observations of low-latitude red auroras at the initial phase of magnetic storms. *Journal of Geophysical Research: Space Physics*, *118*, 256–270. https://doi.org/10.1029/2012JA018001